International Journal for Multidisciplinary Research (IJFMR)

E-ISSN: 2582-2160 ● Website: www.ijfmr.com ● Email: editor@ijfmr.com

Design and Structural Evaluation of a 6-DOF Robotic Arm

Ismail Bogrekci[1], Pinar Demircioglu[2], Erberk Uyar[3]

[1,2]Faculty of Engineering, Department of Mechanical Engineering, Aydin Adnan Menderes University, Aydin, Turkey

[3]Graduate School of Natural and Applied Sciences, Department of Mechanical Engineering, Aydin Adnan Menderes University, Aydin/Turkey & ZF Sachs Süspansiyon Sistemleri A.S., Production-Process Engineer, 41480, Gebze /Turkey

Abstract

This study lays out the design of a robotic arm with six degrees of freedom created to automate the battery swapping operation of unmanned aerial vehicles (UAVs) employed in agriculture. Because UAVs have limited flight capability, the batteries need to be changed frequently, affecting negatively the continuity and efficiency of operations. The robotic arm designed was 3D-modeled in SolidWorks and put through transient structural analyses in Ansys to determine its behavior in actual conditions.

A specially designed cycloidal gear system was incorporated in every joint of the robotic arm for high torque output, low backlash, and compactness. The robot's modular design makes it suitable for different UAV models and mission scenarios. The selection of materials was done considering strength, weight, and manufacturability, and the outer housing is made of aluminum A356, while internal parts are made of 1.8550 steel alloy. The gripper at the end-effector is pneumatically actuated and capable of handling battery modules of up to 12 kg safely.

Inverse kinematics solutions, dynamic simulations, and transient load analyses validated the structural stiffness, low displacement, and high precision of the robotic arm. The findings confirm the effectiveness of the system for field applications, and it is a feasible and novel approach to automated UAV battery replacement in agriculture.

Keywords: Robotic Arm, Cycloidal Gear, UAV, Battery Replacement, Inverse Kinematics, Transient Analysis.

Introduction

Human-robot collaboration has become more popular in recent years [1]. These collaborative robots work alongside human workers in the same workspace and generally employ high-power motors and speed reducers (harmonic drives) to enhance the weight-to-payload ratio. Nevertheless, the utilization of these high-power motors can result in serious harm when there is a collision between a robot and a human is caused by human mistakes or mechanical failures of a robot controller [2]. In addition, the use of high-power motors tends to increase the manufacturing cost of a robot and its power consumption to perform tasks. Thus, a lot of studies have been conducted to minimize the motor torque and power for robot operation. Some researchers applied trajectory planning to minimize torques and energy for robot

operation [5-7], but such trajectories had an adverse effect on the robot performance, and the degree of the minimized torque was comparatively small.
This paper focuses on designing a 6-axis robotic arm to automate battery replacement for UAVs (drones) used in agriculture, aiming to overcome the limitations of manual battery changes and improve operational efficiency. UAVs have become essential in agricultural spraying due to their precision and time-saving benefits, but their limited flight time, constrained by battery capacity, disrupts long-term operations. The proposed robotic arm will provide fast, precise, and automated battery replacement, reducing human dependency.
The design incorporates robust casting materials and custom molds for every part, boosting performance. It utilizes SolidWorks for CAD modeling and Ansys for finite element analysis (FEA) to examine dynamic performance with changing loads. The robotic arm also has a modular design, making it suitable for various UAV models and tasks other than battery replacement, including maintenance procedures.
In the survey by Suomalainen et al., the current state of robotic manipulation tasks involving contact with the environment is presented. Tasks requiring force control and contact strategies are examined. Recent trends are highlighted, where human-performed tasks are increasingly handled by robots with improved generalization, error tolerance, and learning efficiency [3].
In the survey of Jiang et al. [4], the increased application of robotic arms in healthcare, military, and manufacturing fields is reported, motivated by their programmability and intelligence [5,6]. Trajectory tracking, however, is still a problem owing to system complexity, nonlinearity, and exterior disturbances. PID controllers are the most common choice for industrial robots owing to simplicity, but they are plagued by defects such as static error and weak adaptability in nonlinear or uncertain conditions [7]. To overcome these drawbacks, computational intelligence techniques; genetic algorithm, fuzzy logic, and neural network, are introduced, as well as hybrid control strategies [8–10]. Recently, fractional-order PID controllers have demonstrated the ability to enhance control precision and robustness and are a new promising approach for robotic arm trajectory tracking.
The findings and outcome of this comprehensive research represent a very useful and significant reference that will be of great assistance in the development and design of high-precision, multi-functional robotic systems, especially in precision agriculture and other similar autonomous applications.

Material and Method

This section presents materials utilized in constructing the robotic arm, as well as the modeling, simulation, and analysis techniques adopted during the design process and the validation process.
Material selection was based on structural loads, weight, environment, and manufacturability. Two primary materials were selected. Aluminum Alloy A356 was selected for outer housing because it is lightweight, corrosion-resistant, and castable, with a yield strength of ~195 MPa for complicated, non-load-bearing components. 1.8550 Alloy Steel (34CrNiAl7) was chosen for load-bearing elements such as cycloidal discs and shafts due to its high yield strength (~850–950 MPa), excellent wear resistance, and thermal stability. All the material properties (Young's modulus, density, Poisson's ratio) were assigned in the simulation for precise FEA.

A complete parametric 3D CAD model of a 6-axis robot arm was developed. All the joints have a cycloidal drive, and the gripper has a pneumatic system. The assembly encompasses modular joints, built-in motor mounts, internal cable management, and IP-rated seals.

Figure 1 illustrates the front view of the proposed UAV design concept, and Figure 2 shows the isometric view, both of which are used as the foundation for the integration of the robotic arm with UAV platforms.

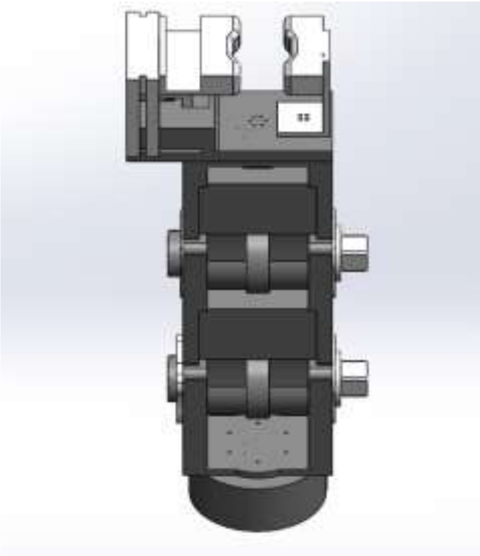

Figure 1: ANOYA UAV Conceptual Design Front View

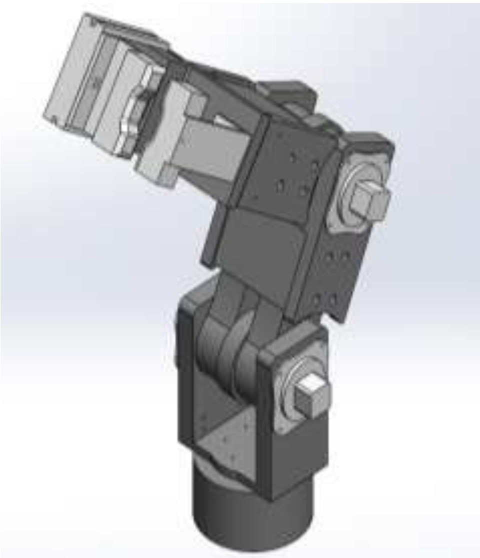

Figure 2: ANOYA UAV Conceptual Design Isometric View

All joints, with the exception of the gripper, were powered by a specially designed cycloidal reducer. The main features are 20-lobe dual-disc, NEMA 17 stepper motor compatibility, backlash-free performance, high torque density, and small size. The isometric and cross-sectional views of the cycloidal gear design illustrate the mechanical advantages and pin layout for torque transmission and accuracy in Figures 3 and 4, respectively.

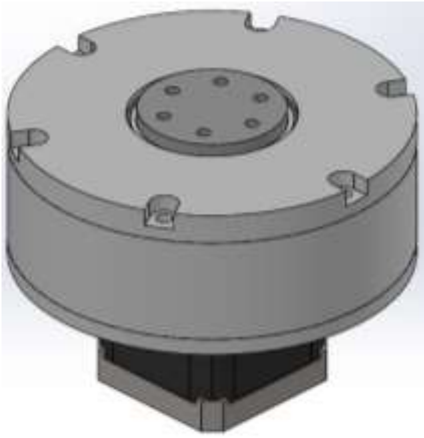

Figure 3: Cycloidal Gear Isometric View

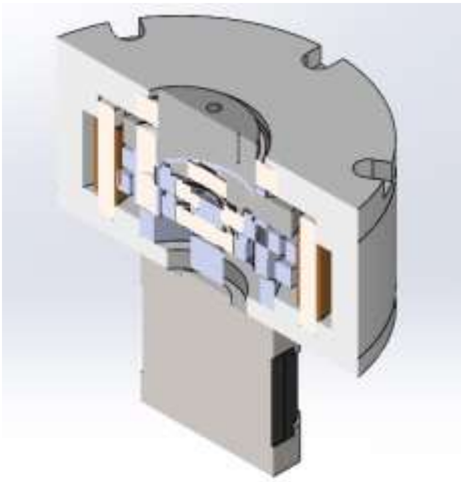

Figure 4: Cycloidal Gear Cross-Sectional View

Each joint, except the gripper, was actuated using a custom-designed cycloidal reducer. Key characteristics include 20-lobe dual-disc configuration, NEMA 17 stepper motor integration, backlash-free operation, high torque density and compact form. These were selected to meet the high precision and load requirements of battery handling applications.

In FEA, transient structural analysis was carried out and as element type, SOLID187 (Tetrahedral) was utilized. In mesh details, average element size ~3–4 mm, mesh convergence confirmed within 2% error margin were chosen. Under boundary conditions, fixed base support was selected, and 12 kg load was applied at gripper. Vertical acceleration of 1.8 m/s² was simulated. According to CAD model (A356 Aluminum and 1.8550 Steel) was assigned.

Forward kinematics was simulated with Denavit–Hartenberg parameters for calculating the end-effector position. Analytical and numerical inverse kinematics solutions were implemented for controlling the pose of the arm. Dynamic behavior was approximated using Lagrangian methods for computing joint torques and inertial effects.

The gripper is driven by a 50 mm stroke pneumatic cylinder and can manage UAV batteries weighing up to 12 kg. It includes 1.8550 steel jaws with polyurethane pads for gripping and accommodates optional proximity and force sensors for feedback. The robotic arm has modular joints for easy part replacement and versatile UAV configurations. The design process incorporated electrical interfaces, motor drivers, and feedback loops for electronic integration in the future. This sensor-integrated and modular architecture guarantees adaptability, maintainability, and readiness for autonomous operation.

Results

The research effectively proved the viability and functionality of a 6-axis robotic arm for automated UAV battery swap in agricultural use. Transient finite element analyses showed that the robotic arm was structurally stable when subjected to dynamic loading, with stresses within the material yield limits of A356 aluminum and 1.8550 steel. Figure 5 shows the von Mises stress distribution under transient loading, confirming that the structure remains well within safe operational limits. Figure 6 depicts the total deformation experienced by the robotic arm during dynamic motion, where the end-effector displacement was below 0.8 mm, satisfying the required precision for reliable battery replacement. These simulation outcomes confirm the structural soundness and dynamic behavior of the robotic arm during actual operating conditions.

To ensure the mechanical robustness and control accuracy of the system, modal analysis was conducted to evaluate the natural frequencies and vibration modes of the robotic arm. Results indicated that the lowest natural frequency was high enough above the arm's operating excitation frequencies, effectively precluding the possibility of resonance during repeated motion cycles.

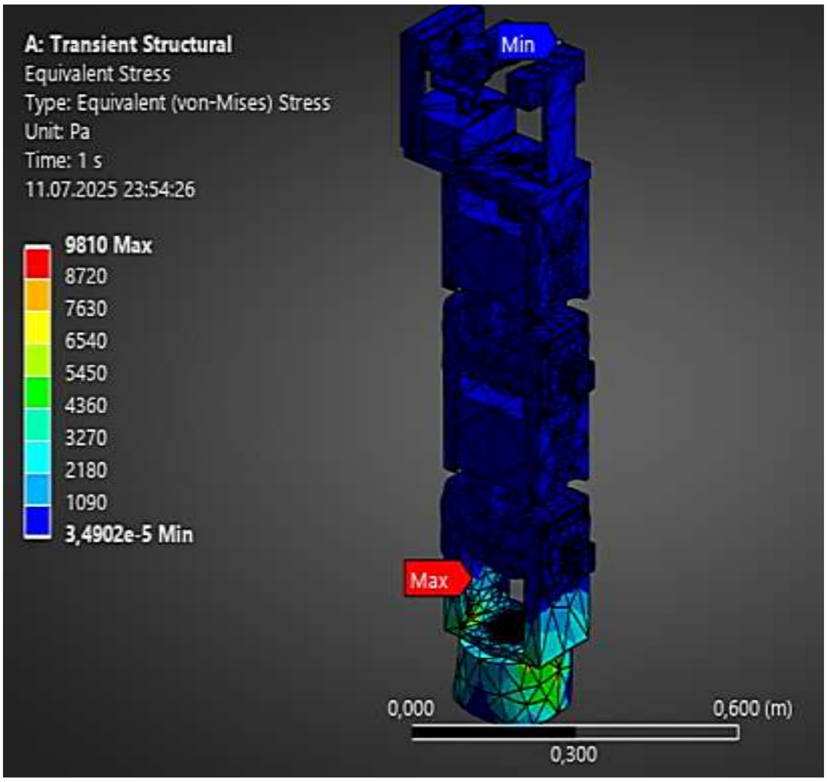

Figure 5: Von-Misses Stress Analyses

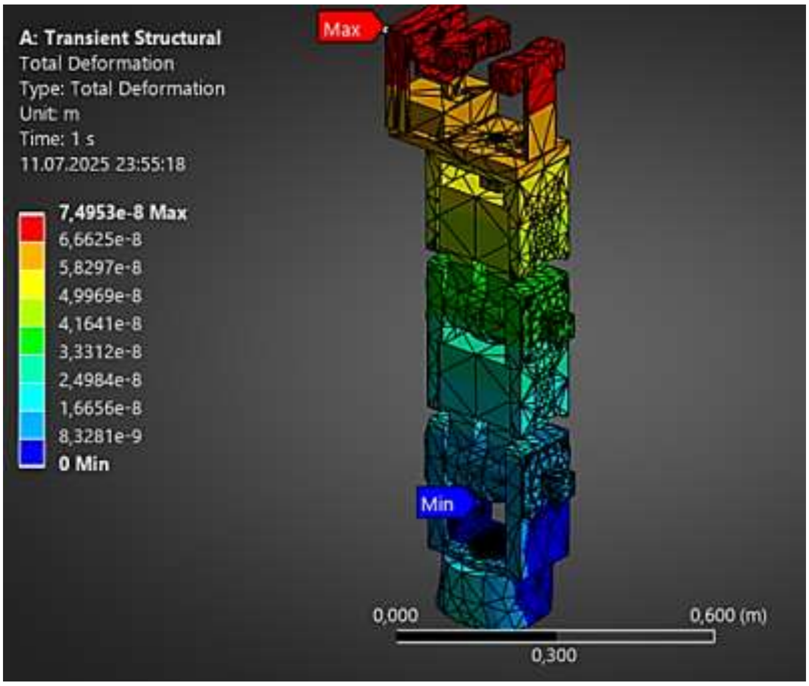

Figure 6: Total Deformation

End-effector total displacement was within 0.8 mm throughout simulated motion sequences, which fulfilled the necessary precision for dependable battery docking procedures. The custom-designed cycloidal gear drives provided high torque output, minimal backlash, and smooth motion transfer, enhancing joint precision and system robustness. The robot arm presented stable performance during simulated acceleration, deceleration, and load change. Joint torques were within the safe operating range of the NEMA 17 stepper motors in conjunction with 20:1 gear reduction. The pneumatic gripper safely manipulated batteries weighing up to 12 kg and precisely matched UAV docking slots through the wrist joint. The modular structure provided adaptability to various sizes of UAVs and facilitated activities such as maintenance and payload management. These results confirm the suggested design as a structurally viable and operationally efficient system for UAV battery replacement automation.

Conclusion

This paper reports on the mechanical design, kinematic modeling, and structural analysis of a 6-degree-of-freedom robotic manipulator for automated UAV battery swapping in agriculture. The primary motivation was to enhance UAV battery life limitations by enabling fast, autonomous battery swaps, increasing uptime and minimizing human intervention in the field.

The robotic arm was modeled in SolidWorks for parametric 3D modeling and verified by transient FEA in ANSYS Workbench 2025. Simulation under realistic dynamic load conditions, e.g., sudden acceleration, payload manipulation, and torque reversal; verified that the mechanical structure ensures high rigidity and position precision. Peak von Mises stress was within 12% of the yield strength of A356 aluminum and 1.8550 steel, and tip deflections were less than 0.8 mm during dynamic maneuvers (as demonstrated in Figures 5 and 6), meeting precision requirements for automated docking operations.

All joints were driven through specially designed cycloidal gear reducers coupled with NEMA 17 stepper motors, enabling compact high-torque transmission with low backlash. The gear trains were optimized for lobe number, reduction ratio (20:1), and contact geometry for smooth motion, load distribution, and structural durability under cyclic loading. The gripper assembly, fabricated from 1.8550 steel and pneumatically actuated, was shown to manipulate payloads up to 12 kg with adaptive grip force and positional compliance.

On the control front, the use of both analytical and numerical inverse kinematics algorithms offered a dual-path solution architecture for path planning and pose control. The analytical method allowed for quick pose resolution for regular configurations, and iterative numerical techniques managed complicated geometries and singularities.

Another major result was the modular design of the robotic system. Every joint was developed as a separate, serviceable module incorporating the drive system, bearings, structural housing, and sensor mounts. The modularity not only enables scalability to various UAV platforms and payload categories but also rapid reconfiguration for other tasks like drone maintenance, payload delivery, or docking interface servicing.

As a conclusion, the robotic system demonstrates high reliability, accuracy, and flexibility. It successfully automates UAV servicing in challenging agricultural environments.

References

1. Lee, W.-B.; Lee, S.-D.; Song, J.-B. Design of a 6-DOF Collaborative Robot Arm with Counterbalance Mechanisms. In Proceedings of the 2017 IEEE International Conference on Robotics and Automation (ICRA); IEEE: Singapore, Singapore, May 2017.
2. *ISO/TS 15066:2016 Robots and Robotic Devices - Collaborative Robots*; **2006**.
3. Suomalainen, M.; Karayiannidis, Y.; Kyrki, V. A Survey of Robot Manipulation in Contact. *Robot. Auton. Syst.* **2022**, *156*, 104224, doi:10.1016/j.robot.2022.104224.
4. Jiang, Z.; Zhang, X.; Liu, G. Trajectory Tracking Control of a 6-DOF Robotic Arm Based on Improved FOPID. *Int. J. Dyn. Control* **2025**, *13*, doi:10.1007/s40435-025-01620-x.
5. Integrated Palletizing Workstation with an Industrial Robot and a Cobot. In *Advances in Intelligent Systems and Computing*; Springer International Publishing: Cham, 2020; pp. 202–209 ISBN 978-3-030-19647-9.
6. Cong, V.D. Visual Servoing Control of 4-DOF Palletizing Robotic Arm for Vision Based Sorting Robot System. *Int. J. Interact. Des. Manuf. IJIDeM* **2023**, *17*, 717–728, doi:10.1007/s12008-022-01077-8.
7. Bae, J.; Moon, Y.; Park, E.; Kim, J.; Jin, S.; Seo, T. Cooperative Underwater Vehicle-Manipulator Operation Using Redundant Resolution Method. *Int. J. Precis. Eng. Manuf.* **2022**, *23*, 1003–1017, doi:10.1007/s12541-022-00685-4.
8. Aydin, M.N.; Coban, R. PID Sliding Surface-Based Adaptive Dynamic Second-Order Fault-Tolerant Sliding Mode Control Design and Experimental Application to an Electromechanical System. *Int. J. Control* **2022**, *95*, 1767–1776, doi:10.1080/00207179.2021.1871963.
9. Khosravi, M.A.; Taghirad, H.D. Robust PID Control of Fully-Constrained Cable Driven Parallel Robots. *Mechatronics* **2014**, *24*, 87–97, doi:10.1016/j.mechatronics.2013.12.001.
10. Shuprajhaa, T.; Sujit, S.K.; Srinivasan, K. Reinforcement Learning Based Adaptive PID Controller Design for Control of Linear/Nonlinear Unstable Processes. *Appl. Soft Comput.* **2022**, *128*, 109450, doi:10.1016/j.asoc.2022.109450.